

# Semantic Edge Detection with Diverse Deep Supervision

Yun Liu<sup>1</sup>, Ming-Ming Cheng<sup>1</sup>, JiaWang Bian<sup>2</sup>, Le Zhang<sup>3</sup>, Peng-Tao Jiang<sup>1</sup>, Yang Cao<sup>1</sup>

<sup>1</sup>Nankai University <sup>2</sup>University of Adelaide <sup>3</sup>Advanced Digital Sciences Center

## ABSTRACT

Semantic edge detection (SED), which aims at jointly extracting edges as well as their category information, has far-reaching applications in domains such as semantic segmentation, object proposal generation, and object recognition. SED naturally requires achieving two distinct supervision targets: locating fine detailed edges and identifying high-level semantics. We shed light on how such distracted supervision targets prevent state-of-the-art SED methods from effectively using deep supervision to improve results. In this paper, we propose a novel fully convolutional neural network architecture using *diverse deep supervision (DDS)* within a multi-task framework where lower layers aim at generating category-agnostic edges, while higher layers are responsible for the detection of category-aware semantic edges. To overcome the distracted supervision challenge, a novel information converter unit is introduced, whose effectiveness has been extensively evaluated in several popular benchmark datasets, including SBD, Cityscapes, and PASCAL VOC2012. Source code will be released upon paper acceptance.

## KEYWORDS

Semantic edge detection, diverse deep supervision

## 1 INTRODUCTION

Classical edge detection aims to detect edges and objects' boundaries. It is *category-agnostic* in the sense that recognizing object categories is not necessary. It can be viewed as a pixel-wise binary classification problem whose objective is to classify each pixel as belonging to one class, indicating the edge, or to the other class, indicating non-edge. In this paper we consider more practical scenarios of semantic edge detection, in which the detection of edges and the recognition of edges' categories within an image is jointly achieved. Semantic edge detection (**SED**) [4, 14, 30, 41] is an active research topic in computer vision due to its wide-ranging applications in problems such as object proposal generation [4], occlusion and depth reasoning [1, 17], 3D reconstruction [33], object detection [11, 12], image-based localization [32] and so on.

Recently, deep convolutional neural networks (DCNNs) reign undisputed as the new de-facto method for category-agnostic edge detection [29, 38] where near human-level performances have been achieved. Deep learning for *category-aware* SED, which jointly detects visually salient edges as well as recognizes their categories, however, is not yet to witness such vast popularity. Hariharan *et al.* [14] first combined generic object detectors with bottom-up edges to recognize semantic edges. A fully convolutional encoder-decoder network is proposed in [39] to detect object contours but without recognizing specific categories. Recently, CASENet [41] introduces a skip-layer structure to enrich category-wise edge activations with bottom layer features, improving previous state-of-the-art methods with a significant margin.

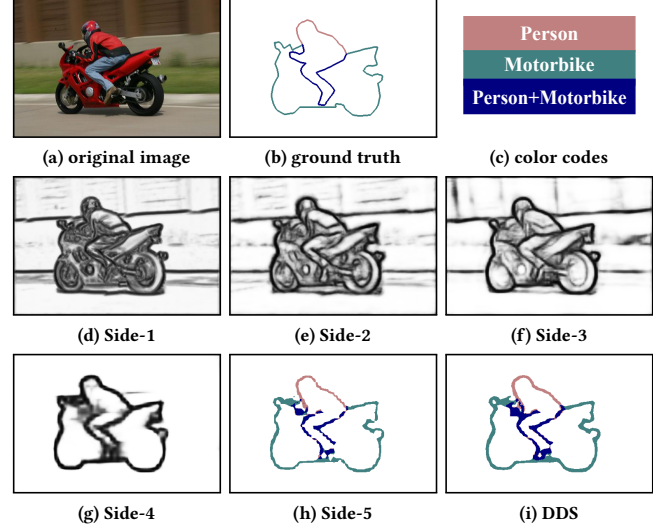


Figure 1: An example of our DDS algorithm. (a) shows the original image from the SBD dataset. (b)–(c) show its semantic edge map and corresponding color codes. (d)–(g) display category-agnostic edges from Side-1–4. (h)–(i) show semantic edges of Side-5 and DDS output, respectively.

**Distracted supervision paradox in SED.** SED naturally requires achieving two distinct supervision targets: i) locating fine detailed edges by capturing discontinuity among image regions, mainly using low-level features; and ii) identifying abstracted high-level semantics by summarizing different appearance variations of the target categories. Such distracted supervision paradox prevents the state-of-the-art SED method, *i.e.* CASENet [41], from successfully applying deep supervision, whose effectiveness has been demonstrated in a wide number of other computer vision tasks, *e.g.* image categorization [36], object detection [26], visual tracking [37], and category-agnostic edge detection [29, 38].

In this paper, we propose a *diverse deep supervision (DDS)* method, which employs deep supervision with different loss functions for high-level and low-level feature learning as shown in Fig. 2(b). While mainly using high-level convolution (*i.e.* **conv**) features for semantic classification and low-level **conv** ones for non-semantic edge details is intuitive and straightforward, directly doing this as in CASENet [41] results in even worse performance than directly learning semantic edges without deep supervision or category-agnostic edge guidance. In [41], Yu *et al.* claimed that deep supervision for lower layers of the network is *not necessary*, after unsuccessfully trying various ways of adding deep supervision. As illustrated in Fig. 2(b), we propose an *information converter* unit for changing the backbone DCNN features into different representations, for training category-agnostic or semantic edges respectively. Without

such information converters, the low-level (*conv* layer 1-4) and high-level (*conv* layer 5) DCNN features would be optimized towards category-agnostic and semantic edges respectively, which can not be easily transformed with simple convolutions between *conv* 4 and *conv* 5 features. By introducing the information converter units, a single backbone representation could be effectively learned end-to-end, towards different targets. An example of our DDS is shown in Fig. 1. The bottom sides of the neural network can help side-5 to find fine details, and thus the final fused semantic edges (Fig. 1 (i)) are smoother than those coming from Side-5 (Fig. 1 (h)).

In summary, our main contributions are:

- Analyzing the distracted supervision paradox in the context of SED task, and why it stops the state-of-the-art SED method [41] from using deep supervision to improve results (Sec. 3).
- Proposing a state-of-the-art SED method, namely *diverse deep supervision* (DDS), which use *information converters* to avoid the difficulties of learning powerful backbone features with distracted supervision (Sec. 4).
- Providing detailed ablation studies to further understand the proposed method (Sec. 5.1).

We extensively evaluate our method on SBD [14], Cityscapes [8], and PASCAL VOC2012 [10] datasets. Our method achieves the new state-of-the-art performance. On the SBD dataset, the average maximum F-measure of our proposed DDS algorithm at optimal dataset scale (ODS) is 73.3%, comparing with previous state-of-the-art performance of 71.4%.

## 2 RELATED WORK

The wealth of research in this area is such that we cannot give an exhaustive review. Instead, we first describe the most important threads of research to solve the problem of classical category-agnostic edge detection, followed by deep learning based approaches, semantic edge detection (SED), and the technique of deep supervision.

**Classical category-agnostic edge detection.** Edge detection has been conventionally solved by designing various filters such as Sobel [35] and Canny [6] to detect pixels with highest gradients in their local neighborhoods. To the best of our knowledge, Konishi *et al.* [21] proposed the first data-driven edge detector in which, unlike previous model based approaches, edge detection was posed as statistical inferences. *Pb* features which consist of brightness, color and texture are used in [31] to obtain the posterior probability of each boundary point. *Pb* is further extended to *gPb* [2] by computing local cues from multi-scale and globalizing them through spectral clustering. Sketch Tokens are learned from hand drawn sketches for contour detection [24]. Random decision forests are employed in [9] to learn the local structure of edge patches and show competitive results among non-deep-learning approaches.

**Deep category-agnostic edge detection.** The number of success stories of machine learning has seen an all-time rise across many computer vision tasks recently. The unifying idea is deep learning which utilizes neural networks aimed at learning complex feature representations from raw data. Motivated by this, deep learning

based methods have made vast inroads into edge detection as well. Ganin *et al.* [13] applied the deep neural network for edge detection using dictionary learning and nearest neighbor algorithm. DeepEdge [3] extracts candidate contour points first and then classifies these candidates. HFL [4] uses SE [9] to generate candidate edge points instead of Canny [6] used in DeepEdge. Compared with DeepEdge which needs to process input patches for every candidate point, HFL turns out to be more computationally feasible as the input image is fed into the network only once. DeepContour [34] partitions edge data into subclasses and fits each subclass by different model parameters. Xie *et al.* [38] leveraged deeply-supervised nets to build a fully convolutional network that performs image-to-image prediction. Their deep model, known as HED, fuses the information from bottom and top *conv* layers. Liu *et al.* [29] introduced the first real-time edge detector that achieves higher F-measure scores than average human annotators on the popular BSDS500 dataset [2].

**Semantic edge detection.** Owing to its strong ability for semantic representation learning, deep learning based edge detectors tend to generate high responses at object boundary locations, *e.g.* Fig. 1 (d)-(g). This inspires research on simultaneously detecting edge pixels and classifying them based on association to one or more of the object categories. The so-called category-aware edge detection is highly beneficial to various vision tasks including object recognition, stereo, semantic segmentation, and object proposal generation.

Hariharan *et al.* [14] first provided a principled way of combining generic object detectors with bottom-up contours to detect semantic edges. Yang *et al.* [39] proposed a fully convolutional encoder-decoder network for object contour detection. HFL produces category-agnostic binary edges and assigns class labels to all boundary points using deep semantic segmentation networks. Maninis *et al.* [30] coupled their convolutional oriented boundaries (COB) with semantic segmentation results by dilated convolutions [40]. A weakly supervised learning strategy is introduced in [19] in which bounding box annotations alone are sufficient to reach high-quality object boundaries without any object-specific annotations. Yu *et al.* [41] proposed a novel network, CASENet, which has pushed SED performance to state-of-the-art. In their architecture, low-level features are only used to augment top classifications. After several failed experiments, they claimed that deep supervision on bottom sides of lower layers is *not necessary* for SED.

**Deep supervision.** Deep supervision has been demonstrated to be effective in many vision or learning tasks such as image classification [23, 36], object detection [25, 26, 28], visual tracking [37], category-agnostic edge detection [29, 38] and so on. Theoretically speaking, lower layers in deep networks learn discriminative features so that classification/regression at higher layers is easier. In practice, one can explicitly influence the hidden layer weight/filter update process to favor highly discriminative feature maps using deep supervision. However, it may not be optimal to directly add deep supervision of category-agnostic edges on the bottom sides because of the distracted supervision discussed above. We will introduce a new semantic edge detector with successful diverse deep supervision in the following sections.

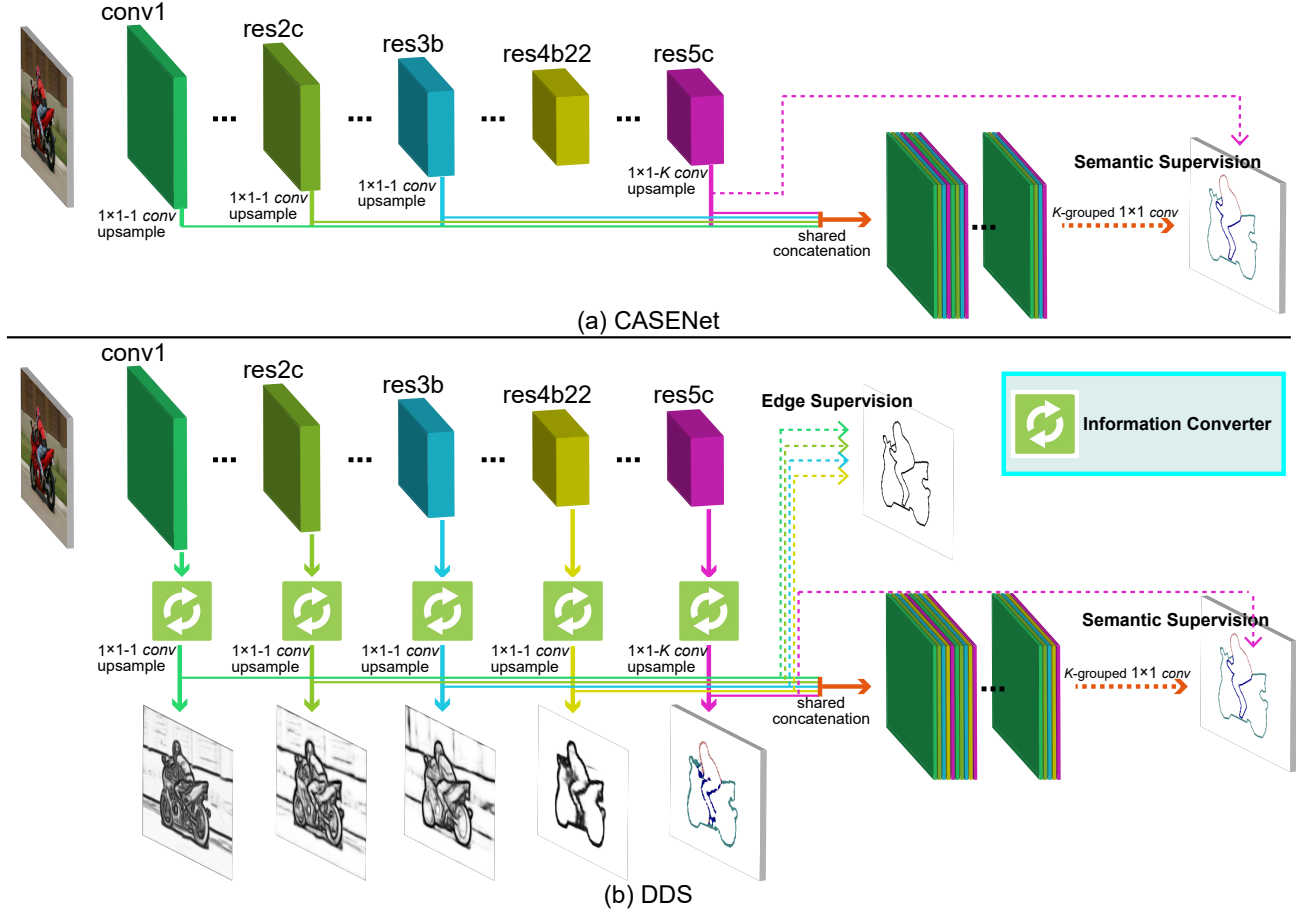


Figure 2: A comparison between two SED models: CASENet [41] and our DDS. CASENet only adds top supervision on the Side-5 activation, and the authors claimed that deep supervision was not necessary in their architecture. However, our proposed DDS network adds deep supervision on all of the side activations. Note that the *information converters* are crucial for avoiding the distracted supervision among category-agnostic and semantic edge detection.

### 3 DISCUSSION OF CASENET

Before expounding on the proposed method, we first briefly introduce the architecture of CASENet [41] in Fig. 2(a).

#### 3.1 CASENet Model

CASENet [41] is built on the well-known backbone network of ResNet [16]. It connects a  $1 \times 1$  conv layer after each of Side-1-3 to produce a single channel feature map  $F^{(m)}$ . The top Side-5 is connected to a  $1 \times 1$  conv layer to output  $K$ -channel class activation map  $A^{(5)} = \{A_1^{(5)}, A_2^{(5)}, \dots, A_K^{(5)}\}$ , where  $K$  is the number of categories. The *shared concatenation* replicates bottom features  $F^{(m)}$  to separately concatenate with each channel of the class activation map:

$$A^f = \{F^{(1)}, F^{(2)}, F^{(3)}, A_1^{(5)}, \dots, F^{(1)}, F^{(2)}, F^{(3)}, A_K^{(5)}\}. \quad (1)$$

Then,  $K$ -grouped  $1 \times 1$  conv is performed on  $A^f$  to generate semantic edge map with  $K$  channels. The  $k$ -th channel represents the edge map for the  $k$ -th category.

#### 3.2 Discussion

CASENet [41] imposes supervision only on Side-5 and the final fused activation. In [41], the authors have tried several deeply supervised architectures. They first separately used all of Side-1-5 for SED and each side is connected a classification loss. The evaluation results are even worse than the basic architecture that directly applies  $1 \times 1$  convolution on Side-5 to obtain semantic edges. It is widely accepted that the lower layers of neural networks contain low-level less-semantic features such as local edges that are not suitable for semantic classification, because the recognition of semantic categories needs abstracted high-level features that appears in the top layers of neural networks. Thus they would obtain poor classification results at bottom sides. Fusing bottom poor results with top results, of course there would not be any improvement for SED accuracy.

They also attempted to impose deep supervision of binary edges on Side-1-3 in CASENet but observed a divergence to the semantic classification at Side-5. With the top supervision of semantic edges, the top layers of the network will be supervised to learn abstracted

high-level semantics that can summarize different appearance variations of the target categories. The bottom layers will be forced to serve the top layers for this goal through back propagation, because the bottom layers are the bases of top layers for the representation power of DCNNs. On the other hand, with the bottom supervision of category-agnostic edges, the bottom layers are taught: all semantic categories are same here, and there only exists the differences between the edge and non-edge. This will cause conflicts at bottom layers and therefore fail to provide discriminative gradient signals for parameter updating.

Note that Side-4 is not used in CASENet. We believe it is a naive way to *alleviate* the information conflicts by regarding the whole *res4* block as a buffer unit between the bottom and top sides. When adding Side-4 to CASENet (see in Sec. 5.1), the new model (*CASENet + Side4*) achieves 70.9% mean F-measure, compared with the 71.4% of original CASENet. This demonstrates our hypothesis about the buffer function of *res4* block. Moreover, the classical  $1 \times 1$  *conv* layer after each side [38, 41] is too weak to buffer the conflicts. In this paper, we propose an information converter unit to solve the conflicts of the distracted supervision.

## 4 OUR APPROACH

Intuitively, employing different but “appropriate” ground-truth for bottom and top sides, the learned intermediate representations of different levels may contain complementary information. But directly imposing deep supervision seems not beneficial here. In this section, we propose a new network architecture for the complementary learning of the bottom and top sides for SED.

### 4.1 The Proposed DDS Algorithm

Based on above discussion, we hypothesize that the bottom sides of neural networks may be not beneficial to SED directly. However, we believe that bottom sides still encode complementary fine details compared with the top side (Side-5). With appropriate architecture re-design, we believe they can be used for category-agnostic edge detection to improve the localization accuracy of semantic edges generated by the top side. To this end, we design a novel *information converter* to assist low-level feature learning and generate consistent gradient signals coming from higher layers. This is essential as they enable directly influencing the hidden layer weight/filter update process to favor highly discriminative feature maps towards correct SED.

We show our proposed network architecture in Fig. 2(b). We follow CASENet to use ResNet [16] as our backbone network. After each of the *information converters* (Sec. 4.2) of Side-1-4, we connect a  $1 \times 1$  *conv* layer with a single output channel to produce an edge response map. These predicted maps are then upsampled to the original image size using bilinear interpolation. These side outputs are supervised by binary category-agnostic edges. We perform  $K$ -channel  $1 \times 1$  convolution on Side-5 to obtain semantic edges, where each channel represents the binary edge map of one category. We adopt the same upsampling operation as done in Side-1-4. Semantic edges are used to supervise the training of Side-5.

Here, we denote the produced binary edge maps from Side-1-4 as  $E = \{E^{(1)}, E^{(2)}, E^{(3)}, E^{(4)}\}$ . The semantic edge map from Side-5 is still represented by  $A^{(5)}$ . A shared concatenation is then performed

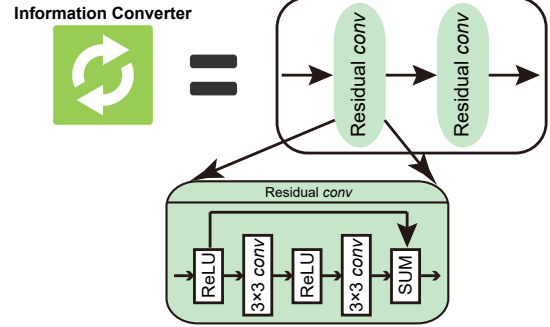


Figure 3: The illustration of our *information converter*.

to obtain the stacked edge activation map:

$$E^f = \{E, A_1^{(5)}, E, A_2^{(5)}, E, A_3^{(5)}, \dots, E, A_K^{(5)}\}. \quad (2)$$

Note that  $E^f$  is a stacked edge activation map, while  $A^f$  in CASENet is a stacked feature map. Finally, we apply  $K$ -grouped  $1 \times 1$  convolution on  $E^f$  to generate the fused semantic edges. The fused edges are supervised by the ground truth of semantic edges. As demonstrated in HED [38], the  $1 \times 1$  convolution can well fuse the edges from bottom and top sides.

### 4.2 Information Converter

Recently, residual nets have been proved to be easier to optimize than plain nets [16]. The residual learning operation is usually embodied by a shortcut connection and element-wise addition. We describe a residual *conv* block in Fig. 3. This block consists of four alternatively connected ReLU and *conv* layers, and the output of the first ReLU layer is added to the output of the last *conv* layer. Our proposed *information converter* combines two residual modules and is connected to each side of DDS network to transform the learned representation into proper form. This operation is expected to avoid the conflicts due to the discrepancy in different loss functions.

The top supervision of semantic edges will produce gradient signals for the learning of semantic features, while the bottom supervision of category-agnostic edges will produce category-agnostic gradients. These conflicting gradient signals will confuse the backbone network through back propagation if the distracted supervision is directly imposed. Our information converters can play a buffer role by converting these conflicting signals into proper representation. In this way, the backbone network will receive consistent update signals and be optimized towards the same target, besides, the different tasks at bottom and top sides are carried out by the *information converters*.

Our proposed network can successfully combine the fine details from the bottom sides and the semantic classification from the top side. The experimental results demonstrate that our algorithm solves the problem of conflicts caused by diverse deep supervision. Unlike CASENet, our semantic classification at Side-5 can be well optimized without any divergence. The produced binary edges from the bottom sides help Side-5 to make up the fine details. Thus the final fused semantic edges can achieve better localization quality.

We use binary edges with single pixel width for the supervision of Side-1-4 and thick semantic boundaries for the supervision of

Side-5 and final fused edges. One pixel is viewed as a binary edge if it belongs to the semantic boundaries of any category. We obtain thick semantic boundaries by seeking the difference between a pixel and its neighbors, like CASENet [41]. A pixel with the label  $k$  is regarded as a boundary of class  $k$  if at least one neighbor with a label  $k'$  ( $k' \neq k$ ) exists.

### 4.3 Multi-task Loss

Two different loss functions, which stand for category-agnostic and category-aware edge detection loss respectively, are employed in our multi-task learning framework. We denote all the layer parameters in the network as  $W$ . Suppose an image  $I$  has a corresponding binary edge map  $Y = \{y_i, i = 1, 2, \dots, |I|\}$ . The sigmoid cross-entropy loss function for Side-1-4 can be formulated as

$$\begin{aligned} L_{side}^{(m)}(W) = & - \sum_{i \in I} [\beta \cdot (1 - y_i) \cdot \log(1 - P(x_i; W)) \\ & + (1 - \beta) \cdot y_i \cdot \log(P(x_i; W))], \quad (3) \\ & (m = 1, \dots, 4), \end{aligned}$$

where  $\beta = |Y^+|/|Y|$  and  $1 - \beta = |Y^-|/|Y|$ .  $Y^+$  and  $Y^-$  represent edge and non-edge ground truth label sets, respectively.  $x_i$  is the produced activation value at pixel  $i$ .  $P(\cdot)$  is the standard sigmoid function.

For an image  $I$ , suppose the semantic ground truth label is  $\{\bar{Y}^1, \bar{Y}^2, \dots, \bar{Y}^K\}$ , in which  $\bar{Y}^k = \{\bar{y}_i^k, i = 1, 2, \dots, |I|\}$  is the binary edge map for the  $k$ -th category. Note that each pixel may belong to the boundaries of multiple categories. We use the multi-label loss as in CASENet:

$$\begin{aligned} L_{side}^{(5)}(W) = & - \sum_k \sum_{i \in I} [\beta \cdot (1 - \bar{y}_i^k) \cdot \log(1 - P(x_i^k; W)) \\ & + (1 - \beta) \cdot \bar{y}_i^k \cdot \log(P(x_i^k; W))], \quad (4) \end{aligned}$$

in which  $x_i^k$  is the activation value for  $k$ -th category at pixel  $i$ . The loss of the fused semantic activation map is denoted as  $L_{fuse}(W)$ . The computation of  $L_{fuse}(W)$  is similar to  $L_{side}^{(5)}(W)$ . The total loss is formulated as

$$L(W) = \sum_{m=1, \dots, 5} L_{side}^{(m)}(W) + L_{fuse}(W). \quad (5)$$

With the total loss function, we can use stochastic gradient descent to optimize all parameters.

### 4.4 Implementation Details

We implement our algorithm using the well-known deep learning framework of Caffe [18]. The proposed network is built on ResNet [16]. We follow CASENet [41] to change the strides of the first and fifth convolution blocks from 2 to 1. The atrous algorithm is used to keep the receptive field sizes the same as the original ResNet. We also follow CASENet to pre-train the convolution blocks on the COCO dataset [27]. The network is optimized with stochastic gradient descent (SGD). Each SGD iteration chooses 10 images uniformly at random and crops a  $352 \times 352$  patch from each of them. The weight decay and momentum are set to 0.0005 and 0.9, respectively. The base learning rate is set to  $5e-7/2.5e-7$  for SBD [14] and Cityscapes [8] datasets, respectively. We use the learning rate policy of “poly”, in which the current learning rate equals the base

one multiplying  $(1 - curr\_iter/max\_iter)^{power}$ . The parameter of  $power$  is set to 0.9. We run 25k/80k iterations of SGD for SBD [14] and Cityscapes [8] datasets, respectively. We use the model trained on SBD to test PASCAL VOC2012 without retraining. The side upsampling operation is implemented with deconvolution layers by fixing the parameters to perform bilinear interpolation. All experiments are performed using a NVIDIA TITAN Xp GPU.

## 5 EXPERIMENTS

We evaluate our method on several datasets, including SBD [14], Cityscapes [8], and PASCAL VOC2012 [10]. SBD [14] comprises 11355 images and corresponding labeled semantic edge maps for 20 Pascal VOC classes. It is divided into 8498 training and 2857 validation images. We use the training set to train our network and the validation set for evaluation. The Cityscapes dataset [8] is a large-scale semantic segmentation dataset with stereo video sequences recorded in street scenarios from 50 different cities. It consists of 5000 images that are divided into 2975 training, 500 validation and 1525 test images. The ground truth of the test set has not been published because it is an online competition. Thus we use the training set for training and validation set for test as on SBD dataset. PASCAL VOC2012 [10] contains the same 20 classes as SBD. Due to the same reason, the semantic labeling of test set has not been published. We generate a new validation set which excludes training images in SBD. This results in 904 validation images. We test on this new set using the models trained on SBD training set to test the generalization ability of different methods.

For evaluation protocol, we use the standard benchmark published in [14]. The maximum F-measure ( $F_m$ ) at optimal dataset scale (ODS) for each class and mean maximum F-measure across all classes are reported. For Cityscapes and VOC2012 datasets, we follow [14] to generate semantic edges with single pixel width, so that the produced boundaries are just the boundaries of *semantic objects or stuff* in semantic segmentation. We also follow [41] to downsample the ground truth and predicted edge maps of Cityscapes into half sizes of original dimensions for the speed of evaluation.

### 5.1 Ablation Study

In this part, we perform some ablation experiments on SBD to first investigate our proposed DDS algorithm in various aspects before comparing with existing state-of-the-art methods. To this end, we propose six DDS variants:

- **Softmax** that only adopts the top side (Side-5) with 21-class softmax loss function, so that the ground truth edges of each category are not overlapping and thus each pixel has one specific class label.
- **Basic** that employs the top side (Side-5) for multi-label classification, which means we directly connect the loss function of  $L_{side}^{(5)}(W)$  on *res5c* to train the detector.
- **DSN** that directly applies the deeply supervised network architecture, in which each side of the backbone network is connected a  $1 \times 1$  conv layer with  $K$  channels for SED and the resulting activation maps from all sides are fused to generate the final semantic edges.
- **CASENet + Side4**, which is similar to CASENet but taking into account Side-4 that connects a  $1 \times 1$  conv layer to produce

**Table 1: The ODS F-measure (%) of ablation methods on the SBD validation set [14].**

Method	aer.	bike	bird	boat	bottle	bus	car	cat	chair	cow	table	dog	horse	mot.	per.	pot.	sheep	sofa	train	tv	mean
Softmax	74.0	64.1	64.8	52.5	52.1	73.2	68.1	73.2	43.1	56.2	37.3	67.4	68.4	67.6	76.7	42.7	64.3	37.5	64.6	56.3	60.2
Basic	82.5	74.2	80.2	62.3	68.0	80.8	74.3	82.9	52.9	73.1	46.1	79.6	78.9	76.0	80.4	52.4	75.4	48.6	75.8	68.0	70.6
DSN	81.6	75.6	78.4	61.3	67.6	82.3	74.6	82.6	52.4	71.9	45.9	79.2	78.3	76.2	80.1	51.9	74.9	48.0	<b>76.5</b>	66.8	70.3
CASENet + Side4	84.1	76.4	80.7	63.7	70.3	81.3	73.4	79.4	56.9	70.7	47.6	77.5	81.0	74.5	79.9	54.5	74.8	48.3	72.6	69.4	70.9
DDS – Converter	83.3	77.1	81.7	63.6	70.6	81.2	73.9	79.5	56.8	71.9	48.0	78.3	81.2	75.2	79.7	54.3	76.8	48.9	75.1	68.7	71.3
DDS – DeepSup	82.5	77.4	81.5	62.4	70.8	81.6	73.8	80.5	56.9	72.4	46.6	77.9	80.1	73.4	79.9	54.8	76.6	47.5	73.3	67.8	70.9
CASENet [41]	83.3	76.0	80.7	63.4	69.2	81.3	74.9	<b>83.2</b>	54.3	74.8	46.4	<b>80.3</b>	80.2	76.6	80.8	53.3	77.2	50.1	75.9	66.8	71.4
DDS	<b>85.4</b>	<b>78.3</b>	<b>83.3</b>	<b>65.6</b>	<b>71.4</b>	<b>83.0</b>	<b>75.5</b>	81.3	<b>59.1</b>	<b>75.7</b>	<b>50.7</b>	80.2	<b>82.7</b>	<b>77.0</b>	<b>81.6</b>	<b>58.2</b>	<b>79.5</b>	<b>50.2</b>	<b>76.5</b>	<b>71.2</b>	<b>73.3</b>

**Table 2: The ODS F-measure (%) of some competitors on the SBD validation set [14].**

Method	aer.	bike	bird	boat	bottle	bus	car	cat	chair	cow	table	dog	horse	mot.	per.	pot.	sheep	sofa	train	tv	mean
InvDet [14]	41.5	46.7	15.6	17.1	36.5	42.6	40.3	22.7	18.9	26.9	12.5	18.2	35.4	29.4	48.2	13.9	26.9	11.1	21.9	31.4	27.9
HFL-FC8 [4]	71.6	59.6	68.0	54.1	57.2	68.0	58.8	69.3	43.3	65.8	33.3	67.9	67.5	62.2	69.0	43.8	68.5	33.9	57.7	54.8	58.7
HFL-CRF [4]	73.9	61.4	74.6	57.2	58.8	70.4	61.6	71.9	46.5	72.3	36.2	71.1	73.0	68.1	70.3	44.4	73.2	42.6	62.4	60.1	62.5
BNF [5]	76.7	60.5	75.9	60.7	63.1	68.4	62.0	74.3	54.1	76.0	42.9	71.9	76.1	68.3	70.5	53.7	<b>79.6</b>	<b>51.9</b>	60.7	60.9	65.4
WS [19]	65.9	54.1	63.6	47.9	47.0	60.4	50.9	56.5	40.4	56.0	30.0	57.5	58.0	57.4	59.5	39.0	64.2	35.4	51.0	42.4	51.9
DilConv [40]	83.7	71.8	78.8	65.5	66.3	82.6	73.0	77.3	47.3	76.8	37.2	78.4	79.4	75.2	73.8	46.2	79.5	46.6	76.4	63.8	69.0
DSN [41]	81.6	75.6	78.4	61.3	67.6	82.3	74.6	82.6	52.4	71.9	45.9	79.2	78.3	76.2	80.1	51.9	74.9	48.0	<b>76.5</b>	66.8	70.3
COB [30]	84.2	72.3	81.0	64.2	68.8	81.7	71.5	79.4	55.2	<b>79.1</b>	40.8	79.9	80.4	75.6	77.3	54.4	82.8	51.7	72.1	62.4	70.7
CASENet [41]	83.3	76.0	80.7	63.4	69.2	81.3	74.9	<b>83.2</b>	54.3	74.8	46.4	<b>80.3</b>	80.2	76.6	80.8	53.3	77.2	50.1	75.9	66.8	71.4
DDS	<b>85.4</b>	<b>78.3</b>	<b>83.3</b>	<b>65.6</b>	<b>71.4</b>	<b>83.0</b>	<b>75.5</b>	81.3	<b>59.1</b>	<b>75.7</b>	<b>50.7</b>	80.2	<b>82.7</b>	<b>77.0</b>	<b>81.6</b>	<b>58.2</b>	<b>79.5</b>	50.2	<b>76.5</b>	<b>71.2</b>	<b>73.3</b>

a single-channel feature map while CASENet only uses Side-1-3 and Side-5.

- **DDS – Converter** that removes the *information converters* in DDS, so that deep supervision is directly imposed after each side.
- **DDS – DeepSup** that removes the deep supervision from Side-1-4 of DDS but remains the *information converters*.

We evaluate these variants and the original DDS and CASENet [41] methods on the SBD validation dataset. The evaluation results are shown in Tab. 1. We can see that *Softmax* suffers from significant performance degradation. Because the predicted semantic edges of neural networks are usually thick and overlapping with other classes, it is improper to assign a single label to each pixel. Thus we apply multi-label loss in Equ. (4). The *Basic* network achieves an ODS F-measure of 70.6%, which is 0.3% higher than *DSN*. This further verifies our speculation in Sec. 3 indicating that features from the bottom layers are not discriminative enough for the task of semantic classification. Besides, CASENet + Side4 performs better than *DSN*. It demonstrates that bottom convolution features are more suitable for binary edge detection. Moreover, the F-measure of CASENet + Side4 is lower than original CASENet. In addition, the improvement from DDS – DeepSup to DDS shows that DDS’ success does not come from more parameters (*conv* layers) but comes from the coordination of deep supervision and *information converters*. Adding more *conv* layers but without deep supervision may make the network more difficult to be convergent. Our conclusion is in line with [41], when compared DDS – Converter with the results of CASENet, which indicates that it is useless to directly add binary edge supervision on bottom sides.

Intuitively, employing different but “appropriate” ground-truth for bottom and top sides may enhance the feature learning in different layers. Upon this, the learned intermediate representations of

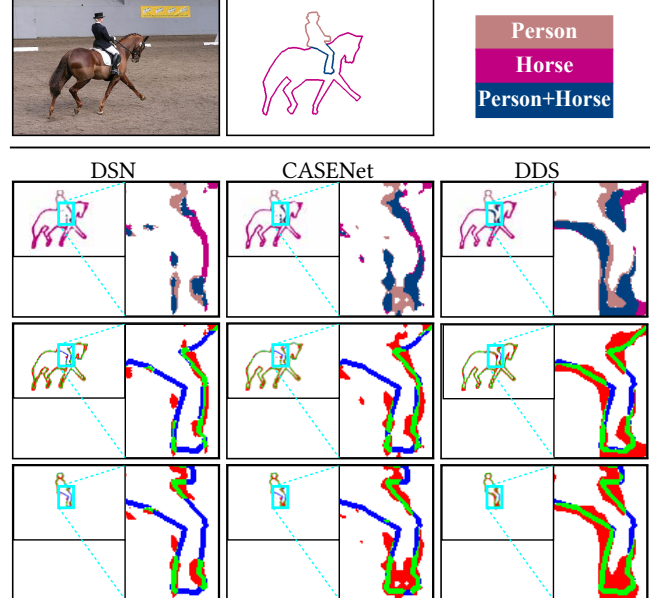


**Figure 4: A qualitative comparison of DSN, CASENet, and DDS. First row: the original image, ground truth, and category color codes. This image is taken from SBD [14] validation set. Second row: the predicted semantic edges of different methods. Third row: The predicted horse boundaries. Green, red, white, and blue pixels represent true positive, false positive, true negative, and false negative points, respectively. Last row: The predicted person boundaries. Best viewed in color.**

**Table 3: The evaluation results (%) of some competitors on the Cityscapes validation set [8].**

Method	road	side.	buil.	wall	fence	pole	light	sign	vege.	terrain	sky	person	rider	car	truck	bus	train	mot.	bike	mean
DSN	85.4	76.4	82.6	51.8	56.5	66.5	62.6	72.1	80.6	61.1	76.0	77.5	66.3	84.5	52.3	67.3	49.4	56.0	76.0	68.5
CASENet	86.6	78.8	85.1	51.5	58.9	70.1	70.8	74.6	83.5	62.9	79.4	81.5	71.3	86.9	50.4	69.5	52.0	61.3	80.2	71.3
DDS	<b>90.5</b>	<b>84.2</b>	<b>86.2</b>	<b>57.7</b>	<b>61.4</b>	<b>85.1</b>	<b>83.8</b>	<b>80.4</b>	<b>88.5</b>	<b>67.6</b>	<b>88.2</b>	<b>89.9</b>	<b>80.1</b>	<b>91.8</b>	<b>58.6</b>	<b>76.3</b>	<b>56.2</b>	<b>68.8</b>	<b>87.3</b>	<b>78.0</b>

**Table 4: The ODS F-measure (%) of some competitors on the VOC2012 validation set [10].**

Method	aer.	bike	bird	boat	bottle	bus	car	cat	chair	cow	table	dog	horse	mot.	per.	pot.	sheep	sofa	train	tv	mean
DSN	83.5	<b>60.5</b>	81.8	58.0	66.4	82.7	69.9	83.0	49.7	78.6	50.8	78.4	74.7	74.1	82.0	55.0	79.9	<b>55.2</b>	78.3	68.6	70.5
CASENet	84.6	60.1	82.7	59.2	68.1	84.3	69.9	<b>83.5</b>	51.9	81.2	50.4	<b>80.4</b>	76.7	74.4	81.9	55.8	<b>82.0</b>	54.9	77.8	67.0	71.3
DDS	<b>86.3</b>	58.2	<b>86.0</b>	<b>60.2</b>	<b>71.6</b>	<b>85.2</b>	<b>72.6</b>	83.0	<b>53.0</b>	<b>82.1</b>	<b>54.0</b>	79.4	<b>77.8</b>	<b>74.9</b>	<b>83.5</b>	<b>57.3</b>	81.7	53.6	<b>79.7</b>	<b>71.0</b>	<b>72.6</b>

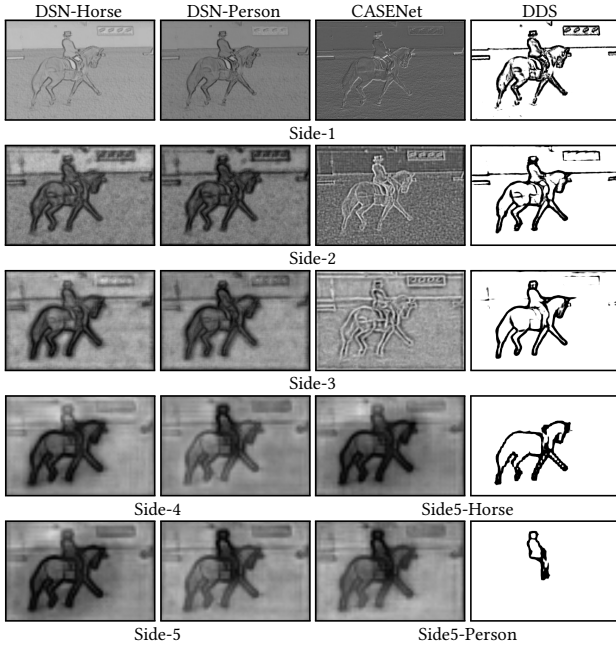


**Figure 5: Side activation maps on the input image of Fig. 4. The first two columns display DSN’s side class classification activations for the classes of horse and person, respectively. The last two columns show the side features of Side-1-3 and class classification activations of Side-5 for CASENet and our DDS, respectively. These images are obtained by normalizing the activations to [0, 255]. Note that all activations are directly outputted without any non-linearization, e.g. sigmoid function.**

different levels tend to contain complementary information. However, in our case, it may not be necessary to directly add deep supervision of category-agnostic edges on bottom sides, because less discriminative gradient signals are likely to be caused by the discrepancy in the loss function of Equ. 5. Alternatively, we show with proper architecture re-design, we are able to employ deep supervision for a significant performance boosting. The *information converters* adopted in the proposed method play a central role in guiding lower layers for category-agnostic edge detection. In this way, low-level edges from bottom layers encode more details which assist top layers towards better localized semantic edges.

They also work well towards generating consistent gradient signals coming from higher layers. This is essential as they enable directly influencing the hidden layer weight/filter update process to favor highly discriminative feature maps towards correct SED.

The significant performance improvement of our proposed DDS over *CASENet + Side4* and *DDS - Converter* demonstrates the importance of our design in which different sides use different supervision after the information format conversion. After exploring DDS with several variants and establishing the effectiveness of the approach, we summarize the results obtained by our method and compare it with several state-of-the-art methods.

## 5.2 Evaluation on SBD

We compare DDS on SBD dataset with several state-of-the-art methods including InvDet [14], HFL-FC8 [4], HFL-CRF [4], BNF [5], WS [19], DilConv [40], DSN, COB [30], and CASENet [41]. Evaluation results are summarized in Tab. 2.

InvDet is a non-deep learning based approach which shows competitive results among other conventional approaches. COB is a state-of-the-art category-agnostic edge detection method. Combining it with semantic segmentation results of DilConv brings a competitive semantic edge detector [30]. The improvement of COB over DilConv reflects the effectiveness of the fusion algorithm in [30]. The fact that both CASENet and DDS outperform COB illustrates that directly learning semantic edges is crucial, because the combination of binary edges and semantic segmentation is not enough for SED. DDS achieves the state-of-the-art performance across all competitors. DDS also outperforms other methods on 15 classes across total 20 classes. The ODS F-measure of our DDS algorithm is 1.9% higher than CASENet and 2.6% higher than COB. Thus DDS pushes the SED to the new state of the art. The average runtime of DSN, CASENet, and DDS is displayed in Tab. 5. Hence DDS can generate state-of-the-art semantic edges only with slightly slower speed.

**Table 5: The average runtime per image on SBD dataset [14].**

Method	DSN	CASENet	DDS
Time (s)	0.171	0.166	0.175

To better view edge prediction results, we show an example in Fig. 4. We also show the normalized images of side activations in Fig. 5. All activations are obtained before sigmoid non-linearization.

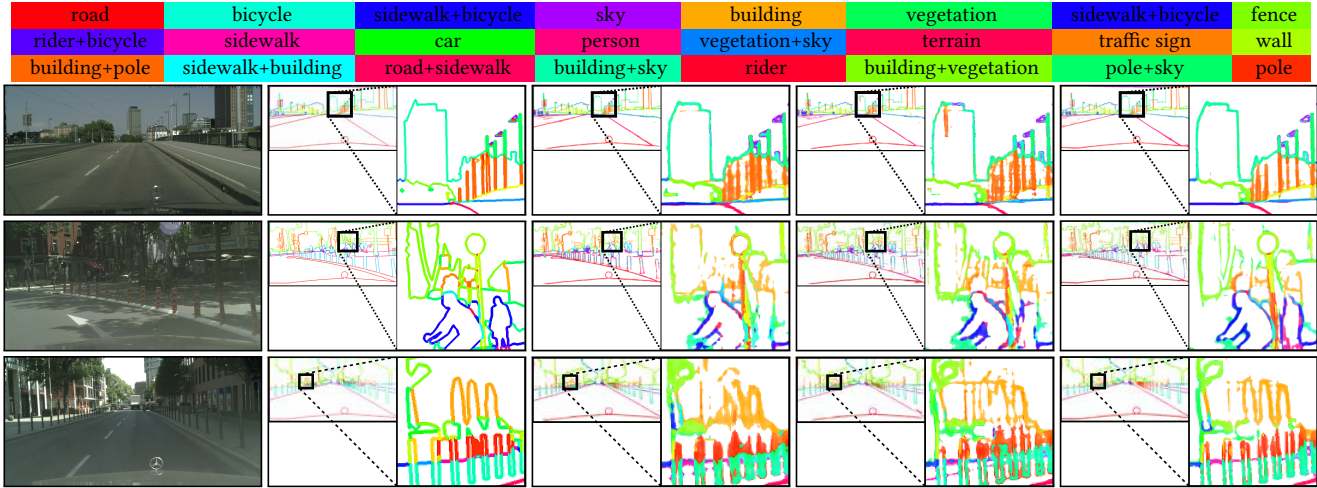


**Figure 6: Some examples from Cityscapes. From left to right: Original image, ground truth, DSN, CASENet and DDS. We can see that the produced edges of DDS are smoother and clearer.**

For the arrangement of the pictures, we do not display Side-4 activation of our DDS. From Side-1 to Side-3, one can see that the feature maps of DDS are significantly clearer than DSN and CASENet. We can find clear category-agnostic edges for DDS, while DSN and CASENet suffer from noisy activations. For example in CASENet, without imposing deep supervision on Side-1-3, we can hardly find its edge activations. For category classification activations, DDS can separate horse and person clearly, while DSN and CASENet can not. Thus the *information converters* also help Side-5 to be better optimized for category-specific classification. This further verifies the feasibility of DDS.

### 5.3 Evaluation on Cityscapes

Cityscapes [8] dataset is more challenging than SBD [14]. The images in Cityscapes are captured in more complicated scenes, usually in the urban street scenes of different cities. There are more objects, especially more overlapping objects in each image. Thus Cityscapes may be better to test semantic edge detectors. We report the evaluation results in Tab. 3. DDS achieves better results than CASENet on all categories. The mean ODS F-measure of DDS is 6.7% higher than CASENet. Some qualitative comparisons are shown in Fig. 6. We can see that DDS can produce smoother and clearer edges.

### 5.4 Evaluation on PASCAL VOC2012

VOC2012 [10] contains the same object categories as SBD [14]. For the validation set, we exclude the images that appear in SBD training set. This results in a new validation set with 904 images. We use the new validation set to test some competitors with the model trained on SBD. By this way, we can test the generalization ability of various methods. However, the original annotations of VOC2012 leave a thin unlabeled area near the boundary of each object. This will lead to an uncertain evaluation. Instead, we follow the methodology in [39] to employ a dense CRF model [22] to fill the uncertain area with the neighboring object labels. We further

follow [14] to generate semantic edges with single pixel width. The evaluation results are summarized in Tab. 4. DDS achieves the best performance, as expected, indicating that DDS has good generalization ability.

## 6 CONCLUSION

In this paper, we study the problem of SED. Previous methods claim that deep supervision in this area is not necessary. We show this is not true and with proper architecture re-design, we are able to deeply supervise the network for better detection results. The core of our approach is the introduction of novel *information converters*, which play a central role in guiding lower layers for category-agnostic edge detection. They also work well towards generating consistent gradient signals with the ones coming from category-aware edge detection in the higher layers. DDS is essential as it enables influencing the hidden layer weight/filter update process directly to favor highly discriminative feature maps towards correct SED. DDS achieves the state-of-the-art performance on several datasets including SBD [14], Cityscape [8], and PASCAL VOC2012 [10]. Our idea to leverage deep supervision for training a deep network opens a path towards putting more emphasis utilizing rich feature hierarchies from deep networks for SED as well as other high-level tasks such as semantic segmentation [7, 30], object detection [11, 30], and instance segmentation [15, 20].

## REFERENCES

- [1] Mohamed R Amer, Siavash Yousefi, Raviv Raich, and Sinisa Todorovic. 2015. Monocular extraction of 2.1 D sketch using constrained convex optimization. *IJCV* 112, 1 (2015), 23–42.
- [2] Pablo Arbeláez, Michael Maire, Charless Fowlkes, and Jitendra Malik. 2011. Contour detection and hierarchical image segmentation. *IEEE TPAMI* 33, 5 (2011), 898–916.
- [3] Gedas Bertasius, Jianbo Shi, and Lorenzo Torresani. 2015. DeepEdge: A multi-scale bifurcated deep network for top-down contour detection. In *IEEE CVPR*. 4380–4389.
- [4] Gedas Bertasius, Jianbo Shi, and Lorenzo Torresani. 2015. High-for-low and low-for-high: Efficient boundary detection from deep object features and its applications to high-level vision. In *IEEE ICCV*. 504–512.

[5] Gedas Bertasius, Jianbo Shi, and Lorenzo Torresani. 2016. Semantic segmentation with boundary neural fields. In *IEEE CVPR*. 3602–3610.

[6] John Canny. 1986. A computational approach to edge detection. *IEEE TPAMI* 6 (1986), 679–698.

[7] Liang-Chieh Chen, Jonathan T Barron, George Papandreou, Kevin Murphy, and Alan L Yuille. 2016. Semantic image segmentation with task-specific edge detection using cnns and a discriminatively trained domain transform. In *IEEE CVPR*. 4545–4554.

[8] Marius Cordts, Mohamed Omran, Sebastian Ramos, Timo Rehfeld, Markus Enzweiler, Rodrigo Benenson, Uwe Franke, Stefan Roth, and Bernt Schiele. 2016. The cityscapes dataset for semantic urban scene understanding. In *IEEE CVPR*. 3213–3223.

[9] Piotr Dollár and C Lawrence Zitnick. 2015. Fast edge detection using structured forests. *IEEE TPAMI* 37, 8 (2015), 1558–1570.

[10] M. Everingham, L. Van Gool, C. K. I. Williams, J. Winn, and A. Zisserman. [n. d.]. The PASCAL Visual Object Classes Challenge 2012 (VOC2012) Results. <http://www.pascal-network.org/challenges/VOC/voc2012/workshop/index.html>. ([n. d.]).

[11] Vittorio Ferrari, Loic Fevrier, Frederic Jurie, and Cordelia Schmid. 2008. Groups of adjacent contour segments for object detection. *IEEE TPAMI* 30, 1 (2008), 36–51.

[12] Vittorio Ferrari, Frederic Jurie, and Cordelia Schmid. 2010. From images to shape models for object detection. *IJCV* 87, 3 (2010), 284–303.

[13] Yaroslav Ganin and Victor Lempitsky. 2014.  $N^4$ -Fields: Neural network nearest neighbor fields for image transforms. In *ACCV*. Springer, 536–551.

[14] Bharath Hariharan, Pablo Arbelaez, Lubomir Bourdev, Subhransu Maji, and Jitendra Malik. 2011. Semantic contours from inverse detectors. In *IEEE ICCV*. IEEE, 991–998.

[15] Zeeshan Hayder, Xuming He, and Mathieu Salzmann. 2017. Boundary-aware Instance Segmentation. In *IEEE CVPR*. 5696–5704.

[16] Kaiming He, Xiangyu Zhang, Shaoqing Ren, and Jian Sun. 2016. Deep residual learning for image recognition. In *IEEE CVPR*. 770–778.

[17] Derek Hoiem, Andrew N Stein, Alexei A Efros, and Martial Hebert. 2007. Recovering occlusion boundaries from a single image. In *IEEE ICCV*. IEEE, 1–8.

[18] Yangqing Jia, Evan Shelhamer, Jeff Donahue, Sergey Karayev, Jonathan Long, Ross Girshick, Sergio Guadarrama, and Trevor Darrell. 2014. Caffe: Convolutional architecture for fast feature embedding. In *ACM MM*. ACM, 675–678.

[19] Anna Khoreva, Rodrigo Benenson, Mohamed Omran, Matthias Hein, and Bernt Schiele. 2016. Weakly supervised object boundaries. In *IEEE CVPR*. 183–192.

[20] Alexander Kirillov, Evgeny Levinkov, Bjoern Andres, Bogdan Savchynskyy, and Carsten Rother. 2017. Instancecut: from edges to instances with multicut. In *IEEE CVPR*. 5008–5017.

[21] Scott Konishi, Alan L. Yuille, James M. Coughlan, and Song Chun Zhu. 2003. Statistical edge detection: Learning and evaluating edge cues. *IEEE TPAMI* 25, 1 (2003), 57–74.

[22] Philipp Krähenbühl and Vladlen Koltun. 2011. Efficient inference in fully connected crfs with gaussian edge potentials. In *NIPS*. 109–117.

[23] Chen-Yu Lee, Saining Xie, Patrick Gallagher, Zhengyou Zhang, and Zhuowen Tu. 2015. Deeply-supervised nets. In *Artificial Intelligence and Statistics*. 562–570.

[24] Joseph J Lim, C Lawrence Zitnick, and Piotr Dollár. 2013. Sketch tokens: A learned mid-level representation for contour and object detection. In *IEEE CVPR*. 3158–3165.

[25] Tsung-Yi Lin, Piotr Dollár, Ross Girshick, Kaiming He, Bharath Hariharan, and Serge Belongie. 2016. Feature pyramid networks for object detection. In *IEEE CVPR*.

[26] Tsung-Yi Lin, Priya Goyal, Ross Girshick, Kaiming He, and Piotr Dollár. 2017. Focal loss for dense object detection. *arXiv preprint arXiv:1708.02002* (2017).

[27] Tsung-Yi Lin, Michael Maire, Serge Belongie, James Hays, Pietro Perona, Deva Ramanan, Piotr Dollár, and C Lawrence Zitnick. 2014. Microsoft coco: Common objects in context. In *ECCV*. Springer, 740–755.

[28] Wei Liu, Dragomir Anguelov, Dumitru Erhan, Christian Szegedy, Scott Reed, Cheng-Yang Fu, and Alexander C Berg. 2016. Ssd: Single shot multibox detector. In *European conference on computer vision*. Springer, 21–37.

[29] Yun Liu, Ming-Ming Cheng, Xiaowei Hu, Kai Wang, and Xiang Bai. 2017. Richer Convolutional Features for Edge Detection. In *IEEE CVPR*. 3000–3009.

[30] Kevis-Kokitsi Maninis, Jordi Pont-Tuset, Pablo Arbelaez, and Luc Van Gool. 2017. Convolutional Oriented Boundaries: From Image Segmentation to High-Level Tasks. *IEEE TPAMI* (2017).

[31] David R Martin, Charless C Fowlkes, and Jitendra Malik. 2004. Learning to detect natural image boundaries using local brightness, color, and texture cues. *IEEE TPAMI* 26, 5 (2004), 530–549.

[32] Srikumar Ramalingam, Sofien Bouaziz, Peter Sturm, and Matthew Brand. 2010. Skyline2gps: Localization in urban canyons using omni-skylines. In *IEEE\RSJ IROS*. IEEE, 3816–3823.

[33] Qi Shan, Brian Curless, Yasutaka Furukawa, Carlos Hernandez, and Steven M Seitz. 2014. Occluding contours for multi-view stereo. In *IEEE CVPR*. 4002–4009.

[34] Wei Shen, Xinggang Wang, Yan Wang, Xiang Bai, and Zhiqiang Zhang. 2015. DeepContour: A deep convolutional feature learned by positive-sharing loss for contour detection. In *IEEE CVPR*. 3982–3991.

[35] Irwin Sobel. 1970. *Camera models and machine perception*. Technical Report. Stanford Univ Calif Dept of Computer Science.

[36] Christian Szegedy, Wei Liu, Yangqing Jia, Pierre Sermanet, Scott Reed, Dragomir Anguelov, Dumitru Erhan, Vincent Vanhoucke, and Andrew Rabinovich. 2015. Going deeper with convolutions. In *Proceedings of the IEEE conference on computer vision and pattern recognition*. 1–9.

[37] Lijun Wang, Wanli Ouyang, Xiaogang Wang, and Huchuan Lu. 2015. Visual tracking with fully convolutional networks. In *IEEE ICCV*. 3119–3127.

[38] Saining Xie and Zhuowen Tu. 2015. Holistically-nested edge detection. In *IEEE ICCV*. 1395–1403.

[39] Jimei Yang, Brian Price, Scott Cohen, Honglak Lee, and Ming-Hsuan Yang. 2016. Object contour detection with a fully convolutional encoder-decoder network. In *IEEE CVPR*. 193–202.

[40] Fisher Yu and Vladlen Koltun. 2016. Multi-scale context aggregation by dilated convolutions. In *ICLR*.

[41] Zhiding Yu, Chen Feng, Ming-Yu Liu, and Srikumar Ramalingam. 2017. CASENet: Deep Category-Aware Semantic Edge Detection. In *IEEE CVPR*. 5964–5973.